OPERATION OF THE UVSOR-II FEL IN HELICAL MODE

M. Labat, CEA Saclay - 91 191 Gif-sur-Yvette, France
M.E. Couprie, Synchrotron SOLEIL - 91 192 Gif-sur-Yvette, France
M. Shimada, M. Katoh, UVSOR Facility - Okazaki, Japan
M. Hosaka, Nagoya University - Nagoya, Japan

Abstract

Seeded Free Electron Lasers (FELs) - an external laser source is injected inside the undulator to perform energy modulation of the electron beam - deliver intense, short duration, short wavelength light pulses with a high temporal coherence degree. Since the polarization of the radiation depends on the undulator magnetic field, the FELs operated with adjustable undulators are unique candidates for providing flexible polarized light of high quality, required for probing symmetry properties of matter. Experiments have been performed on the UVSOR-II storage ring FEL in the seeded Coherent Harmonic Generation (CHG) scheme operated with helical undulators. The electron beam stored at 500 MeV is seeded using a 800 nm Ti:Sa laser, allowing radiation at 400 nm (second harmonic). A quarter wave plate allows the tuning of the polarization of the seeded laser from linear to elliptic or circular. We show that the FEL radiation intensity can be significantly improved via the seed polarization matching. Other parameters of optimization are also presented, such as the focussing mode. The experimental results are analysed using a simple 1D analytical model.

INTRODUCTION

Free Electron Lasers (FELs) in the Self Amplified Spontaneous Emission (SASE) [1] or High Gain Harmonic Generation configurations (HGHG) [2] provide ultrashort femtosecond VUV to X-rays wavelength radiation for investigations on molecular dynamics, atomic motion or structural changes, as well as exploration of physical properties of material. In addition, operated with adjustable undulators, FELs can provide a flexible polarized light of high quality, which is highly requested for probing symmetry properties of matter [3, 4, 5].

FELs are based on the amplification of an optical wave by a relativistic electron beam wiggling inside an undulator. In SASE configuration, the optical wave, provided by the spontaneous emission of the electrons, grows exponentially along a large number of undulator sections, until saturation is reached. In HGHG case, an external source is injected inside a first undulator to modulate the beam, enabling coherent radiation in the next undulators. This last configuration is more compact and provides higher quality radiation in terms of coherence and shot to shot stability [6]. Coherent Harmonic Generation FELs on storage rings [7, 8], thus in small signal gain, also consist in injecting a laser source inside a first undulator for energy modulation of the re–circulating beam, which then, after passing through a dispersive section, emits in a second undulator coherent radiation with harmonic content. CHG and HGHG FELs share key technical issues such as spatial and temporal adjustment of the overlap of the two beams inside the first undulator, as well as theoretical issues such as the effect of seeding on the FEL coherence properties and nonlinear harmonic generation. Therefore, investigations in CHG configuration on the present storage rings is of high interest in the perspective of operating next generation FELs for critical users experiments.

A CHG FEL is implemented on UVSOR-II storage ring [9] (Okazaki, Japan) using an external infra–red laser source as a seed [10]. The performed experiments aim at improving the general understanding of CHG FELs operated with helical undulators, the required mode of operation for users experiments with circular polarized radiation. In this paper, after a brief description of the experimental setup, we show that the FEL radiation intensity can be significantly improved via the seed laser polarization and focussing mode.

EXPERIMENTAL SETUP

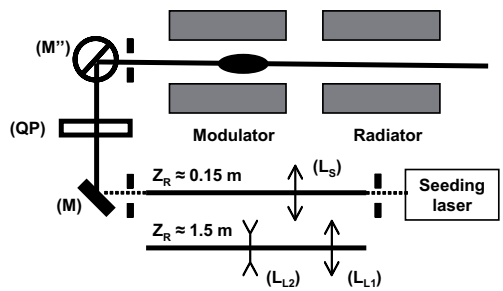

Figure 1: General layout of the CHG experiment on UVSOR-II storage ring. (L_S): 5 m focussing lens, (L_{L1}): 1 m focussing lens, (L_{L2}): 0.5 m defocussing lens. Seeding laser waist position: at the end of the modulator. (QP): quarter wave plate. (M): flat mirror. (M"): periscope consisting of two flat mirrors. The other parameters are given in Table 1, 2 and 3

The experimental setup for the operation of the CHG FEL on UVSOR-II storage ring is given in Fig. 1. The electron beam is stored in single–bunch mode at 500 MeV in the high emittance mode. The beam parameters are given in Table 1.

Table 1: Electron beam parameters for the CHG experiment on UVSOR-II storage ring.

Parameter	Symbol	Value
Energy (MeV)	E	500
Ring circumference (m)	C	53.2
RF frequency (MHz)	f_{RF}	90.1
Harmonic number	h	16
Number of bunch stored		1
Revolution period (ns)	T_{rev}	176
Horizontal emittance (nm.rad)	ϵ_x	84
Vertical emittance (nm.rad)	ϵ_y	4.2
Relative energy spread (%)	σ_γ	0.028

Table 2: Optical klystron parameters for the CHG experiment on UVSOR-II storage ring.

Parameter	Symbol	Value
Number of undulator periods	N	9
Undulator period (cm)	λ_0	11
Dispersive section length (cm)		33
Gap range (mm)	g	35-230
Polarization		Variable

The interaction with the laser takes place in an optical klystron [11] which consists of two undulators separated by a dispersive section. Thanks to translation stages on the permanent magnets lanes, the undulators can be either planar or helical [12, 13]. In the experiment presented here, the undulators are positioned in the helical mode, which sets the output radiation polarization to circular. Because of mechanical constraints, both undulators are tuned at the same resonant wavelength, which corresponds to the seeding laser wavelength, and the dispersive section strength is fixed. To fulfil the resonance condition with the seeding laser, operation of the optical klystron in helical configuration requires a deflection parameter K of 3.8 with a beam of 500 MeV. The optical klystron parameters are given in Table 2.

The seeding laser is focussed inside the first undulator of the OK, and performs energy modulation of the electron beam. Two modes of focussing are used. One single lens of f=5 m focussing length enables a strong focussing in the undulator, corresponding to a short Rayleigh length of Z_R=0.15 m. A f=1 m focussing lens together with a f=-0.5 m defocussing lens allow a smoother focussing corresponding to a Rayleigh length of Z_R=1.5 m. In addition, a quarter wave plate is used to modify the natural polarization. The angle between the incident radiation and the neutral axis of the plate, θ, sets the final seeding laser polarization which can be varied from linear to circular. The laser parameters are given in Table 3. For the modulation to be efficient, the laser is aligned on the electron beam path in the modulator using the last two mirrors and synchronized with the electron beam revolution in the ring [10].

Table 3: Seeding laser parameters for the CHG experiment on UVSOR-II storage ring.

Parameter	Symbol	Value
Wavelength (nm)	λ_L	800
Pulse energy (mJ)	E_L	2
Pulse duration (ps- FWHM)	ΔT_L	0.15 to 1.2
Repetition rate (kHz)	f_{rep}	1
Average power (W)	P_L	2
Beam diameter (mm)	Φ_L	12
Polarization		Horizontal

The output radiation of the optical klystron consists of the spontaneous emission, the coherent harmonics generated and the residual seeding laser light. The radiation is transported to an optical table via three aluminum mirrors, and sent to various photodetectors depending on the wavelength to be analyzed. For measurement of the second harmonic, a visible photomultiplier is used (Hamamatsu, R928), and two band pass filters centered on 405 nm (VPF-25C-40-40-4000 with 39 nm bandwidth fwhm, and Corion P10405A-H972 with 10 nm fwhm bandwidth) provide spectral selection. Because of the diameter of the second band pass filter (less than 10 mm), the measured radiation corresponds to an angular aperture of 1 mrad. A lens (SLSQ-30-200P, focus length of 20 cm) further focusses the radiation inside the detection window of the photomultiplier. The photodetector signal is sent to an oscilloscope triggered by the 1 kHz laser system, which enables to visualize the emission of the interacting bunch among the non interacting ones.

OBSERVATION OF THE COHERENT HARMONICS

In the high emittance mode, the FEL gain [14] is low (0.08%), limiting the observation of coherent radiation up to the third harmonic. In this work, we concentrate on the analysis of the (stronger) second harmonic. Fig. 2 presents a typical example of the photomultiplier signal in CHG operation. The central peak corresponds to the bunch emission when the laser is seeded and edged peaks to the bunch emission when the laser is off. The interaction of the laser and electron beams in the modulator leads to the generation of additional coherent photons in the radiator, causing the strong enhancement of the bunch emission (central peak).

OPTIMIZATION OF THE CHG FEL

We now investigate on the influence of various parameters on the FEL properties operated with helical undulators. Fig. 3 shows the intensity of the second coherent harmonic as a function of the polarization angle θ of the quarter wave plate (angle between the incident polarization and the neutral axis of the plate). When θ is null, the laser keeps its initial linear polarization. In this case, the second coherent

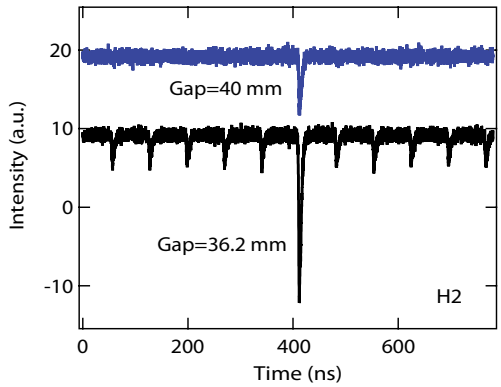

Figure 2: Intensity of the second harmonic. Seeding laser parameters: P_L=1.5 W, ΔT_L=1.2 ps–fwhm with circular polarization. I=2.8 mA.

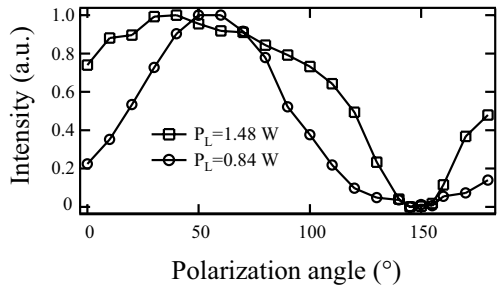

Figure 3: Normalized intensity of the second coherent harmonic as a function of the polarization angle θ. Z_R=1.5 m with (○) P_L= 0.84 W and (□) P_L= 1.48 W.

harmonic is generated but with a low intensity. The maximum intensity is reached when the seeding laser polarization is circular, i.e. for θ=135^o. When the seeding laser polarization is circular in the opposite direction (θ=45^o), the intensity falls to zero: coherent emission is no longer observed. Finally, when the polarization is ellipsoidal, the intensity remains below the maximum. The coherent emission intensity dependency observed on the seeding laser polarization can be simply explained using a 1D analytical model.

In helical configuration, the magnetic field $\vec{B}$ inside the optical klystron is:

$$B_x = B_{ox} cos(k_0 z) \qquad (1)$$
$$B_y = -B_{oy} sin(k_0 z).$$

The first Lorentz equation gives the expression of the transverse electron beam velocity:

$$\beta_x = \frac{K}{\gamma} cos(k_0 z) \qquad (2)$$
$$\beta_y = -\frac{K}{\gamma} sin(k_0 z).$$

The seeding laser electric field $\vec{E}_L$ is initially linear polarized and can be expressed as:

$$E_{Lx} = E_L cos(k_L z - \omega_L t + \phi_0)$$
$$E_{Ly} = 0$$

After passing through the quarter wave plate, the field $\vec{E}_L$ becomes:

$$E_{Lx} = E_L sin(\theta) cos(k_L z - \omega_L t + \phi_0) \qquad (3)$$
$$E_{Ly} = E_L cos(\theta) sin(k_L z - \omega_L t + \phi_0),$$

The seeding laser polarization remains linear for $\theta = 0$, $\frac{\pi}{2}$ and π, becomes circular for $\theta = \frac{\pi}{4}$ and $\frac{3\pi}{4}$, and ellipsoidal for intermediate values.

The second Lorentz equation allows the calculation of the normalized energy exchange inside the modulator:

$$\Delta\gamma = -\frac{ec}{mc^2} \int_{L_{int}} \vec{E}_L . \vec{\beta}_e dt \qquad (4)$$

Using Eq.(2) and (3) in Eq.(4) and with t expressed as a function of z: $t = c\beta_{ez} z$, E_{ech} becomes:

$$E_{ech} = -\frac{eE_L K}{\gamma mc^2 \beta_{ez}} \times$$
$$\int_{L_{int}} [sin(\theta) cos(k_0 z) cos(k_L \frac{1+K^2}{2\gamma^2} z + \phi_0)$$
$$-cos(\theta) sin(k_0 z) sin(k_L \frac{1+K^2}{2\gamma^2} z + \phi_0)] dz \qquad (5)$$

The energy exchange as a function of the polarization of the seeding laser via θ can now be calculated. The evolution of $\Delta\gamma(\theta, E_L)$ as a function of θ calculated using (Eq.(5)) is presented in Fig. 4. As observed experimentally, the energy exchange responsible for coherent emission is maximum for θ=135^o, corresponding to a circular polarization of the laser in the same direction as the magnetic field. When the polarization is in the opposite direction, the energy exchange is null, resulting in the absence of coherent emission.

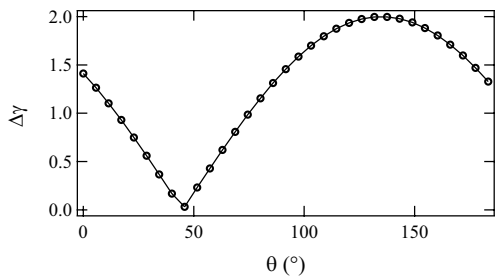

Figure 4: Normalized energy exchange $\Delta\gamma$ as a function of the polarization angle θ of the seeding laser. Calculation using Eq.(5) with σ_L=1 ps–FWHM, $E_L = 3.98 \times 10^8$ V/m and other parameters of Table 1, 2 and 3.

The intensity of the second harmonic, still as a function of the polarization angle θ, has also been measured for various seed laser power and the short focussing mode, as illustrated in Fig. 5. The width at half-maximum of the plots $\Delta\theta$ increases with the seeding power. In addition, the top of

the plots becomes flat. Indeed, the intensity of the coherent emission I_{coh} depends on the energy exchange as:

$$I_{Coh} \propto J_n^2(4n\pi(N+N_d)\frac{\Delta\gamma(\theta,E_L)}{\gamma}) \quad (6)$$

J_n being the Bessel function of order n and N_d the number of equivalent periods of the dispersive section. And the energy exchange depends on the seeding power P_L via the laser electric field as: $E_L \propto \sqrt{P_L}$. Therefore, the coherent intensity depends on the seeding laser power via the argument of the Bessel function. Such function is not continuously increasing but reaches a maximum. Once this maximum passed, J_n and consequently I_{coh} decreases. When the seeding power is too high, the electron beam is overmodulated and the coherent emission is degraded. Since the maximum energy exchange $\Delta\gamma$ is obtained with a circular polarization, a slight misadjustment, i.e. an ellipsoidal polarization, limits the energy exchange and allows to compensate the too strong seeding power and to recover the maximum coherent intensity. As observed experimentally, the optimum polarizations with a strong seeding power are slightly displaced from the circular polarization, which results in a broadening of the plots.

The focussing mode drives similar effect: using a strong focussing (see Fig. 5) leads to larger $\Delta\theta$ than using a smooth focussing (see Fig. 3). Indeed, the energy exchange terms depends on the focussing via the electric field as: $E_L \propto Z_R^{-1/2}$. A decrease of Z_R results in an increase of the electric field and consequently of the Bessel function argument, which can results in an overmodulation of the electronic distribution and further decrease of the coherent emission.

The analysis of Fig. 3 and Fig. 5 reveals that the seeding laser parameters (polarization, power and focussing mode) enable to optimize the coherent intensity via a control of the electron bunch modulation in the modulator. Since the temporal coherence of the FEL depends on the quality of the microbunching in the radiator, those parameters are also expected to enable optimization of the coherence properties of the FEL.

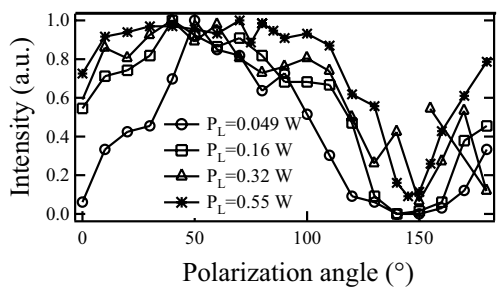

Figure 5: Normalized intensity of the second coherent harmonic as a function of the polarization angle θ. Z_R=0.15 m with ($\circ$) P_L= 0.049 W, ($\square$) P_L= 0.16 W, (Δ) P_L= 0.32 W, ($*$) P_L= 0.55 W.

CONCLUSION

In this paper, we detailed the operation of a CHG FEL with helical undulator. We show that the seeded FEL can be optimized using the seeding laser polarization. The experiment has been performed on a storage ring based seeded FEL, i.e. in the small gain regime. Nevertheless, since the optimization concerns the energy exchange in the modulator, the results can be extended to the LINAC based high gain FELs which will deliver XUV radiation of high quality within very short pulses. Seeded FELs operated with helical undulators appear as unique candidates for the next generation flexible polarization light sources.

REFERENCES

[1] B. Bonifacio et al., Opt. Commun. **50**, 373 (1984).

[2] L.H. Yu et al., Phys. Rev. **A 44**, 5178 (1991).

[3] L. Young and al., Phys. Rev. Lett. **97**, 083601 (2006).

[4] J. Vogel and al., Appl. Phys. Lett. **82**, 2299 (2003).

[5] L. Nahon and al., Applied Optics **43**, 1024 (2004).

[6] L.H. Yu et al., Nucl. Inst. Meth. **A 528**, 436-442 (2004).

[7] R. Coisson and F. De Martini, Phys. of Quant. Electron. **9**, 939 (1982)

[8] R. Prazeres et al., Nucl. Inst. Meth. **A 272**, 68 (1988)

[9] M. Katoh, M. Hosaka, A. Mochihashi, J. Yamazaki, K. Hayashi, Y. Hori, T. Honda, K. Haga, Y. Takashima, T. Koseki, S. Koda, H. Kitamura, T. Hara, T. Tanaka, Proceedings of the AIP'04 Conference **708**, 49-52 (2004).

[10] M. Labat et al., Eur. Phys. J. **D 44**, 187200 (2007)

[11] N.A. Vinokurov and A.N. Skrinsky, Preprint **77-59**, Nuclear Physics Institute of Novossibirsk (1977).

[12] H. Hama, Nucl. Instr. Meth. **A 375**, 57 (1996).

[13] H. Hama, K. Kimura, M. Hosaka, J. Yamazaki, T. Kinishita, Nucl. Instr. Meth. **A 393**, 23 (1997).

[14] P. Elleaume, Optical Klystron, J. Phys. (Paris) **44** C1-353 (1983).